Biosensors and Bioelectronics 40 (2013) 271–276

Contents lists available at SciVerse ScienceDirect

Biosensors and Bioelectronics

journal homepage: www.elsevier.com/locate/bios

Casein modified gold nanoparticles for future theranostic applications

Marisol Espinoza-Castañeda [a], Alfredo de la Escosura-Muñiz [a], Gemma González-Ortiz [b], Susana M. Martín-Orúe [b], José Francisco Pérez [b], Arben Merkoçi [a,c,*]

[a] Nanobioelectronics & Biosensors Group, CIN2 (ICN-CSIC), Catalan Institute of Nanotechnology, Campus UAB, Bellaterra (Barcelona), Spain
[b] Nutrition, Management and Welfare Research Group, Animal and Food Science Department, Universitat Autònoma de Barcelona, Barcelona, Spain
[c] ICREA, Barcelona, Spain

ARTICLE INFO

Available online 27 July 2012

Keywords:
Gold nanoparticle
Biosensor
Bacteria
Caseinglycopeptide
Caseinglycomacropeptide
Hydrogen evolution electrocatalysis
Theranostic

ABSTRACT

The synthesis and characterization of gold nanoparticles (AuNPs 20 nm sized) modified with k-casein derived peptides in order to monitor the peptide effect as bacterial adhesion inhibitor, thanks to the carrier/concentrator effect of the AuNPs is here presented. Some aspects related to the stability of AuNP/peptide conjugates for a potential application in the design of an electrochemical biosensor for pathogen bacteria detection are also discussed. This peptide based nanoparticle assay takes advantage of the dual character of the AuNPs: as carrier of the biorecognition molecule and also as electrocatalytic label, allowing the evaluation of the pathogen bacteria–peptide interaction in a simple and rapid way through the chronoamperometric monitoring of the hydrogen evolution reaction on screen-printed carbon electrodes. The developed proof of concept theranostic system may open the way to therapeutic and biosensing applications with interest for various fields.

1. Introduction

Nanomaterials (NMs) play an important role in current sensing and biosensing technologies. These materials are showing improvement of the performance of biosensing systems in general i.e. for the detection of proteins (De la Escosura-Muñiz et al., 2010a), cells (Perfézou et al., 2011), heavy metals (Aragay et al., 2011) and that of electrochemical sensing devices particularly. In addition to the biosensing applications (De la Escosura-Muñiz et al., 2008; Merkoçi, 2010; Pérez-López and Merkoçi, 2011), the use of nanoparticles (NPs) as carriers of biomolecules and their application in biomedical and nutritional technologies, between others, is an emerging research field in the last years. It is well known that NPs exhibit physical properties that are truly different from both small molecules and bulk material (Dreaden et al., 2012). The special properties of NPs are due to their high ratio between surface area/total volume and the high surface energy, allowing a strong biomolecules adsorption. These biomolecules can be used in order to carry the nanoparticles to the target organ and/or the biomolecules by themselves can exert therapeutic effects (Mohanraj and Chen, 2006). Gold nanoparticles (AuNPs) are specially suitable for such applications, due to their low toxicity (Xue et al., 2011) and good biocompatibility with peptides, proteins, DNAs, etc. (Xu et al., 2006). These nanomaterials can be synthesized reproducibly, modified with seemingly limitless chemical functional groups, and in certain cases, characterized with atomic-level precision, (Giljohann et al., 2010).

Thanks to the combination of all these properties, AuNPs have been extensively proposed for applications in several fields such as the environmental and the food/agriculture one (Huang et al., 2011; Dykman and Khlebtsov, 2012; Jans and Huo, 2012) being especially relevant their application for biomedical and therapeutic purposes (Merkoçi, 2010). Functional nanomaterials show different modalities for treatment of common diseases such as cancers (Peer et al., 2007; Barreto et al., 2011; Yang et al., 2012), abnormal blood vessel growth (Chauhan et al., 2012), and infectious diseases (Blecher et al., 2011).

Among potential target diseases for functional nanomaterials are the enteric diseases, in both humans and animals. While infants diarrhea is a major cause of mortality in developing countries, enteric diseases is also a leading cause of mortality in piglets and a major cause of economic losses in the pig industry (Madec et al., 2000). Enterotoxigenic *E. coli* (ETEC) K88 is the main bacterial cause of diarrhea in piglets around weaning and the adhesion of ETEC to the intestinal mucosa is a prerequisite step for its colonization. Specifically, *E. coli* F4, K88 serotype expresses fimbrial adhesions which specifically identifies affinities to glycoproteins, sialoglycoproteins or glycosphingolipids in the membrane of host cells (Sharon and Gallagher, 2009; Shoaf-Sweeney and Hutkins, 2009). Recently, different authors have suggested that the dietary inclusion of some receptor analogs, on the basis of their glycoside composition, would be a practical strategy to reduce the number of some

* Corresponding author at: Institut Català de Nanotecnologia, ETSE-Edifici Q, 2ª planta, Campus UAB, 08193 Bellaterra (Barcelona) Spain. Tel.: +34 935868014; fax: +34 935868020.
E-mail address: arben.merkoci@icn.cat (A. Merkoçi).

0956-5663/$ - see front matter © 2012 Elsevier B.V. All rights reserved.
http://dx.doi.org/10.1016/j.bios.2012.07.042

intestinal pathogens that bind to the animal cells via carbohydrate-specific adhesions (Lane et al., 2010).

The casein glycomacropeptide (CGMP), a glycoprotein originated during cheese manufacture, has shown promising effects on the interaction with the microbiota through the activity of carbohydrate moieties present in the molecule (sialic acid content of around 4.2%, (Nakano et al., 2007)). Some authors have reported that CGMP binds the cholera toxin of *Vibrio cholera* (Kawasaki et al., 1992) and inhibits the adhesion of pathogenic *E. coli* to the mucosal surface or its growth in vitro (Malkoski et al., 2001) and *in vivo* and even it has anti-cariogenic properties (Aimutis, 2004). In addition CGMP may also interfere with the host cells, and has been shown to affect both innate and adaptive immunity, modulating the immune/inflammatory response by the activation of macrophages, down-regulation of IL-6 and up-regulation of IL-10 (de Medina et al., 2010).

In the present study, we have combined the ability of the AuNPs to act as, as both carriers/electrocatalytic labels, with the properties of k-casein derived peptides to bind specific bacteria fimbriae adhesions. These peptides modified nanoparticles are used for the evaluation of the interaction between the peptides and the K88 fimbriae bacteria (K88) and found with interest for future potential applications not only for biosensing purposes but also for therapeutic ones. Such a theranostic platform can also be extended to other biotechnological applications including food, health and pharmaceutical fields.

2. Experimental section

2.1. Apparatus and electrodes

Zeta potential of the AuNPs and peptide/AuNPs conjugates was determined with a Malvern Zetasizer Nano-ZS (Malvern Instruments Ltd., UK) according to the manufacturer's recommendations.

Optical characterizations of the AuNPs and peptide/AuNPs conjugates were performed using a Transmission Electron Microscope (TEM) Jeol JEM-2011 (Jeol Ltd, Japan) and a Gemini SpectraMax M2e Multi-Mode Microplate Reader (Molecular Devices, CA, USA).

The electrochemical transducers used were homemade screen-printed carbon electrodes (SPCEs), consisting of three electrodes: working electrode, reference electrode and counter electrode in a single strip fabricated with a semi-automatic screen-printing machine DEK248 (DEK International, Switzerland). The reagents used for this process were: Autostat HT5 polyester sheet (McDermid Autotype, UK) and Electrodag 423SS carbon ink, Electrodag 6037SS silver/silver chloride ink and Minico 7000 Blue insulating ink (Acheson Industries, The Netherlands). (See the detailed SPCE fabrication procedure and pictures of the obtained sensors in the supplementary material, Fig. S1).

An ultrasonic bath (JP Selecta, Spain) was used for the bacteria/peptide/AuNP conjugate pre-treatment before the electrochemical measurements.

The electrochemical measurements were taken using a CompactStat potentiostat (Ivium Technologies, The Netherlands) connected to a PC. All the measurements were carried out at room temperature with a working volume of 50 μL, which was enough to cover the three electrodes contained in the SPCEs connected to the potentiostat by a homemade edge connector module.

2.2. Reagents and solutions

Caseinoglycopeptide (CGP) was purchased from Sigma-Aldrich (Spain) and dissolved in 0.01 M PBS, pH 6.8. Lacprodan (CGMP-10) was purchased from Arla Foods Ingredients (Denmark) and its solutions were prepared in 0.01 M PBS, pH 7.4.

Hydrogen tetrachloroaurate (III) trihydrate ($HAuCl_4 \cdot 3H_2O$, 99.9%) and trisodium citrate ($Na_3C_6H_5O_7 \cdot 2H_2O$) reagents used for the gold nanoparticles preparation were also purchased from Sigma-Aldrich (Spain). KH_2PO_4 and K_2HPO_4 reagents used for the preparation of the phosphate buffer solutions (PBS) were acquired from Fluka (Spain).

An *E. coli* K88 fimbriae bacteria (K88) isolated from a colibacillosis outbreak in Spain serotype (O149:K91:H10 [K-88]/LT-I/STb) was provided by the *E. coli* Reference Laboratory, Veterinary Faculty of Santiago de Compostela (Spain). A non-fimbriated *E. coli* (F4-, F6-, F18-, LT1-, ST1-, ST2+, Stx2e-) (NF) isolated from the feces of a post-weaning piglet was donated by the Department of Animal Health and Anatomy of the Universitat Autònoma de Barcelona (Spain). *E. coli* K88 was cultured in unshaken Luria Broth (Sigma, St Louis) at 37 °C while the *E. coli* NF was cultured shaking the media. Cultures were serially passage every 48 h, at least three times.

All chemicals were used as received and all aqueous solutions were prepared in Milli-Q water.

Safety precautions necessary to work with this bacterium were followed during all the preparation and measurements steps in the lab.

2.3. Methods

2.3.1. Preparation of gold nanoparticles and modification with peptides

20 nm gold nanoparticles (AuNPs) were synthesized by reducing tetrachloroauric acid with trisodium citrate, a method pioneered by Turkevich et al. (1951). A total of 200 mL of 0.01% $HAuCl_4$ solution were boiled with vigorous stirring. 5 mL of a 1% trisodium citrate solution were added quickly to the boiling solution. When the solution turned deep red, indicating the formation of gold nanoparticles, it was left stirring and cooling down. In this way, a dispersed solution of AuNPs was obtained. The size of the obtained AuNPs follows a Gaussian distribution as evaluated by TEM analysis, being the main value (and its deviation) of 20.5 ± 2.2 nm (see Supplementary Material, Fig. S2). In order to facilitate the reading these AuNP are mentioned as "20 nm" NPs along the text.

The conjugation of AuNPs with CGP was performed adapting the procedure reported by Liu and Guo, (2009) where it is described that the critical micelle concentration of casein is around 1.0 mg/mL in 0.01 M PBS pH 6.8. Considering this, different mixtures of CGP in the above mentioned buffer and AuNPs solution (from the obtained stock solution of around 3 nM concentration) were prepared at different ratios. Concretely, three different concentrations of CGP (1, 0.1 and 0.01 mg/mL) and three different CGP/AuNPs concentration ratios (1:1, 1:3 and 3:1) were assayed. The incubations of the CGP/AuNPs solutions were performed in a final volume of 500 μL at 20 °C for 30 min with gentle mixing. Finally, in order to remove the excess of CGP, the conjugate was centrifuged 1× at 14,000 rpm (25 °C) and re-suspended in 500 μL of 0.01 M PBS pH 6.8.

In the case of the CGMP-10 peptide, a similar procedure was followed but using 0.01 M PBS, pH 7.4 as buffer and only a fixed condition: a 0.01 mg/mL concentration of peptide and a CGMP-10/AuNP concentration ratio of 3:1.

2.3.2. TEM analysis with negative staining

3 μL of uranyl acetate were added to 3 μL of the peptide/AuNPs conjugates previously placed on the carbon grill. After 1 min, the excess of acetate was removed with filter paper and dried at room temperature. For comparison purposes, this pre-treatment was also applied for the AuNPs without peptides modification.

2.3.3. Zeta potential measurements

1 mL suspension of AuNPs (the same as for the peptide/AuNP conjugates) was transferred into a 1 mL polystyrene cuvette (DTS1061, Malvern Instruments Ltd). The data were collected and analyzed with the Dispersion Technology software 4.20 (Malvern) producing diagrams for the zeta potential as a distribution versus total counts.

2.3.4. UV–vis spectroscopic measurements

300 μL suspension of AuNPs (the same as for the peptide/AuNP conjugates) were introduced in a well of a microplate and the optical density in the range between 400–600 nm was read with a microplate reader and analyzed using the SoftMax Pro 5.2 program.

2.3.5. E. coli bacteria culture

Both *E. coli* bacterial cells, K88 and NF, from an overnight culture were harvested by centrifuging 15 mL broth volume (5 min, 1700 g). All the supernatants were removed and 0.01 M PBS buffer, at the convenient pH, was added to the cell pellets to achieve an optical density of the bacterial suspensions of 1.30, 1.15 and 1 (650 nm) that corresponds with log 10, log 9 and log 8 CFU/mL, respectively.

2.3.6. Incubation of the peptide/AuNPs conjugates with E. coli bacteria

The incubation was carried out by mixing 500 μL of the peptide/AuNP conjugate with 500 μL of *E. coli* (both K88 and NF) at log 8, log 9 and log 10 CFU/mL during 30 min at 37 °C under gentle stirring. After that, the solution was centrifuged at 1700 g (20 °C, 5′) the supernatant was removed and the pellet re-suspended in 50 μL of 0.01 M PBS buffer (at the pH convenient for each peptide, as detailed in Section 2.2). All the assays were performed in triplicate.

2.3.7. Electrocatalytic detection

50 μL of the bacteria/peptide/AuNP conjugate (different concentrations of bacteria, as detailed in the previous section) were mixed with 50 μL of 2 M HCl and treated in an ultrasonic bath for 5 min. 50 μL of this solution were placed onto the surface of the electrochemical transducer and kept there for 2 min. After that, quantitative analyses were carried out taking advantage of the chronoamperometric mode (De la Escosura-Muñiz et al., 2009, 2010b). Chronoamperograms were obtained by subsequently holding the working electrode at a potential of +1.35 V for 1 min and then applying a negative potential of −1.00 V for 100 s, recording the cathodic current generated. A compromise between the time of analysis and the reproducibility of the cathodic current measured was found for measurements done within 100 s so the absolute value of the current registered at this time was chosen as analytical signal. For shorter times, a higher irreproducibility of the results was found.

The background was recorded for 50 μL of 1 M HCl. A new electrode was employed for each measurement.

3. Results and discussion

3.1. Optimization/characterization of peptide/AuNPs conjugates

The mechanism of the peptide immobilization onto the surface of the AuNPs consists in a physical adsorption (Walstra, 1999; Liu and Guo, 2009). The pH plays here an important role since changes in its value give rise to a variation in the charge of the formed cells which consequently affects their adsorptive properties (Jiang et al., 2005; Liu and Guo, 2009). For this reason, the two peptides (CGP and CGMP-10) assayed in this work were dissolved in 0.01 M PBS buffer at different pHs (6.8 and 7.4 respectively).

The critical micelle concentration (defined as the solute concentration at which micelles first appear in solution [Reis et al., 2004]) of casein is also a crucial parameter to be considered since the micelles can either encapsulate the AuNPs or form agglomerates. For this reason, the concentrations of peptides assayed were below this value, as described in the *methods* section.

Following the experimental procedure detailed in the *methods* section, stable suspensions of both CGP/AuNPs and CGMP-10/AuNPs conjugates were obtained. In order to check the AuNPs surface modification after the conjugation, these suspensions were evaluated following different characterization techniques.

They were first characterized by TEM analysis using a negative staining pre-treatment. Negative staining is an established method, often used in diagnostic microscopy, for contrasting a thin specimen with an optically opaque fluid. Typical stainers are ammonium molybdate, uranyl acetate, uranyl formate, phosphotungstic acid, osmium tetroxide, osmium ferricyanide or auroglucothionate because they scatter electrons well and easily adsorb onto biological matter. Due to these properties, this method is used to view viruses, bacteria, bacterial flagella, biological membrane structures and proteins or protein aggregates, which all have a low electron-scattering power. For this reason, this sample pre-treatment was chosen in order to observe the presence of the peptides around the AuNPs in the prepared conjugates.

As detailed in *methods* section, first of all different CGP peptide concentrations and different CGP/AuNPs conjugation ratios were assayed. A summary of the TEM images obtained under these different conditions and the proposed conjugate configurations are shown in the supplementary material, finding that the optimum conditions corresponded to a CGP concentration of 0.01 mg/mL and a CGP:AuNPs concentration ratio of 3:1. Under these conditions, the agglomeration induced by micelles as well as the encapsulation of the AuNPs inside the micelles are avoided (both phenomena are observed for higher peptide concentrations, as shown in the supplementary material; see Fig. S2). Under these optimum conditions, a good AuNPs dispersion along with a "dark shadow" around them is noticed, as can be observed in Fig. 1A, left; this shadow is not observed for the unmodified AuNPs (Fig. 1A, right).

Furthermore, the size of CGP/AuNPs conjugates is higher (27.9 ± 2.4 nm) in comparison to the non-modified AuNPs (20.5 ± 2.2 nm) (see details of the AuNPs sizes distribution at the Supplementary Material). Both observations suggest an efficient coating by the peptide under these conditions, chosen as optimal and applied also for the conjugation of the CGMP-10 peptide with AuNPs.

The conjugates prepared with both peptides under the above mentioned optimized conditions were also evaluated by UV–vis spectroscopy. As observed in Fig. 1B, a shift in the wavelength of the maximum of absorbance from 520 nm (AuNPs) to 525 nm (CGP/AuNPs) and to 523 nm (CGMP-10/AuNPs) is noticed. Comparing this shift with that reported before (Liu and Guo, 2009), it can be evidenced that the surface of the AuNPs has been modified, suggesting again the conjugate formation.

Finally, zeta potential technique was also used for the characterization of the optimized conjugate. This technique has been recently reported as an efficient tool which allows the monitoring and analysis of chemical modifications on the surface of nanoparticles, with minimal sample preparation (Thielbeer et al., 2011). The easily measurable zeta potential has been used to obtain information concerning the particle surface charge, chemical modifications and also stability of colloid suspensions. A high zeta potential (positive or negative) confers stability since the solution or dispersion resists aggregation. When the absolute

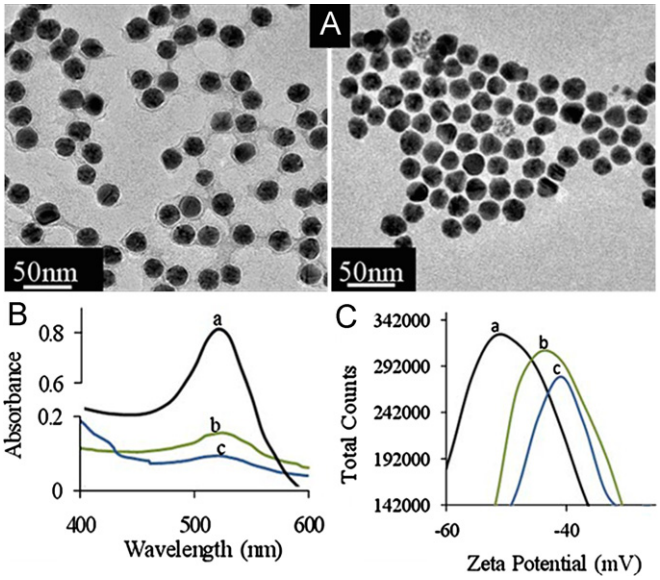

Fig. 1. (A) TEM image (after negative staining pre-treatment) obtained for a CGP/AuNPs suspension prepared following the experimental procedure detailed in the *methods* section (left) and an unmodified AuNPs suspension (right). (B) UV–vis spectra obtained for: (a) AuNPs, (b) CGP/AuNPs and (c) CGMP-10/AuNPs. (C) Diagram for the zeta potential as a distribution versus total counts for: (a) AuNPs, (b) CGP/AuNPs and (c) CGMP/AuNPs.

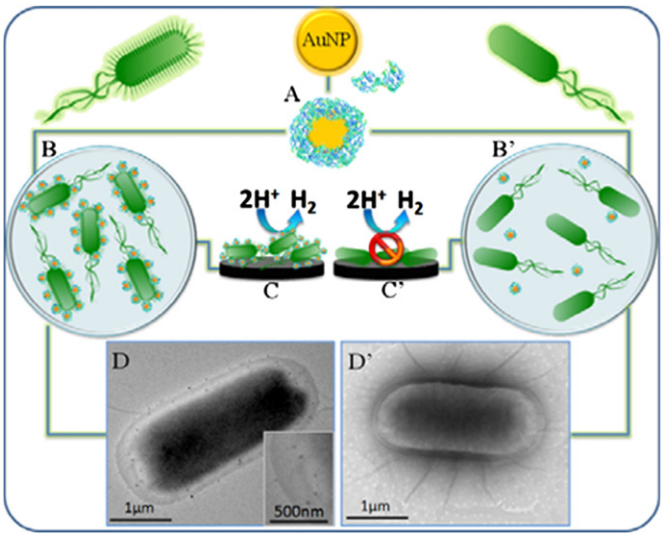

Fig. 2. Schematic representation of the steps involved in the experimental procedure. Peptide/AuNPs conjugates are formed (A), incubated with both fimbriae (K88) (B) and non-fimbriae (NF) (B') *E. coli* and finally detected/discriminated in screen-printed carbon electrodes through the AuNPs electrocatalyzed hydrogen evolution reaction (C, C'). TEM images correspond to K88 (D) and NF (D') *E. coli* after their incubation with the CGP/AuNPs conjugate. The inset image is a zoom that shows AuNPs (small black points) on the surface of the K88 bacteria.

value of the zeta potential is low, attraction exceeds repulsion and the dispersion breaks and flocculates. Due to all that, it has been defined that nanoparticle suspensions begin to be stable for absolute zeta potential values higher than 10 mV. As can be observed in Fig. 1C, the surface charge of the AuNPs reaches a maximum at −52.2 mV, indicating a very good stability of the obtained suspension. When the AuNPs are coated by CGP (CGP/AuNPs) or by CGMP-10 (CGMP-10/AuNPs) a change in the surface charge is noticed through the shift in the value to −44.7 mV and −40.9 mV respectively, indicating again the conjugate formation.

3.2. *Electrocatalytic evaluation of the peptide/AuNP interaction with fimbriated bacteria*

Once the peptide/AuNPs conjugates were formed, their interaction with a fimbriated *E. coli* (K88) was evaluated. As explained before, it is known that some peptides such as k-casein derived ones (this is the case of CGP and CGMP-10) are potential inhibitors of bacterial adhesion to intestinal mucous, being this of potential application in nutritional treatments in order to avoid serious digestive affections, mainly thanks to their ability to bind cholera and *E. coli* enterotoxins. It is proposed that such interaction takes place via the specific adhesion factors (fimbriae) of the bacteria (responsible of the colonization of the small intestine) (Sun et al., 2000), so a non-fimbriae one (NF) was used as control to check the selectivity of the assay.

The interaction of both CGP/AuNPs and CGMP-10/AuNPs conjugates with both kinds of bacteria was studied under the experimental conditions detailed in the *methods* section (see also a scheme of this procedure in Fig. 2A, B, B').

The final electrochemical identification is performed thanks to the electrocatalytic effect of the AuNPs on the electrocatalytic hydrogen evolution reaction on screen-printed carbon electrodes (De la Escosura-Muñiz et al., 2009) (Fig. 2C,C'). The presence of the AuNPs on the electrode surface catalyzes the reduction of hydrogen ions (present in the acidic electrolyte) to hydrogen. This hydrogen evolution generates a cathodic current that can be chronoamperometrically monitored, being the absolute value of the current registered at 100 s (previously optimized) the analytical signal which is proportional to the quantity of AuNPs and, consequently, to the quantity of bacteria. This electrochemically evaluated interaction takes also advantage of the ability of the AuNPs to act as carriers of a high number of peptides which in turns can increase their attachment to K88, ensuring an amplified signal useful for both identification and quantification of bacteria. It is important to mention that, obviously the conjugate is destroyed by the acidic pH used in the final detection step. The use of various acidic mediums after a biological reaction step is, in fact, a common procedure for the detection of nanoparticles (either for their total dissolution or as electrolytic medium), used as labels for both DNA and protein detection(De la Escosura-Muñiz et al., 2008). It is assumed that the biological systems are denaturized, but nanoparticles are still present in the detection solution and their concentration is correlated to the amount of analyte (DNA, protein, bacteria) to be tested.

First of all, the CGP/AuNP was assayed, not observing any catalytic current for both bacteria (data not shown), suggesting that there was not any affinity of this peptide for the bacteria.

However, when the CGMP-10/AuNPs conjugate was assayed, a significant catalytic current was registered, being its value considerably higher for the assay performed with the K88 bacteria in comparison with the obtained for the NF one. As it observed in Fig. 3, the value of this analytical signal is bacteria concentration-dependent in the range of log 10 − log 8 CFU/mL, allowing to discriminate in all cases both kinds of bacteria.

The observed non-specific signals coming from the NF bacteria remain approximately constant for all the assayed concentrations. This behavior seems to indicate that these non-specific signals can be probably due to remaining of peptide/AuNPs not efficiently removed after their incubation with the bacteria (related to low efficiency of the centrifugation/purification step). Anyway even under such experimental conditions a clear discrimination between the two kinds of bacteria can be observed.

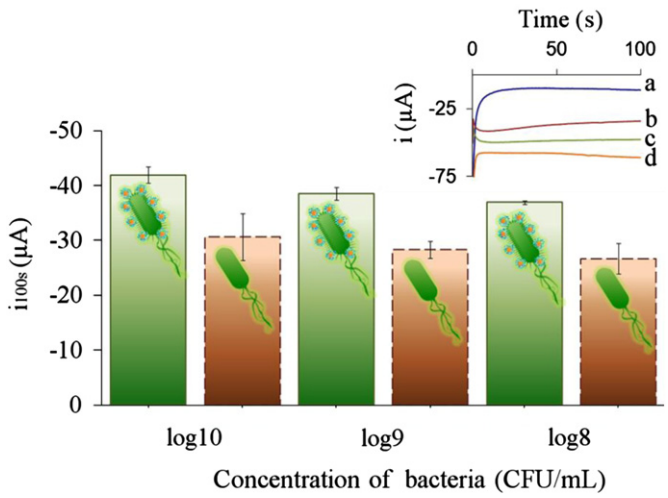

Fig. 3. Summary of the analytical signals (value of the chronoamperometric current at 100 s) obtained for different concentrations of K88 (columns with solid line) and NF (columns with dotted line) bacteria after their incubation with the CGMP-10/AuNPs conjugate, following the experimental procedure detailed at methods section. The inset graph corresponds to the chronoamperograms obtained during the electrocatalytic hydrogen evolution at −1 V in 1 M HCl for a log 10 CFU/mL concentration of K88 (c) and NF (b) after incubation with CGMP-10. For comparison purposes, the background 1 M HCl (a) and the register obtained for AuNPs in 1 M HCl (d) are also shown.

The electrochemical results were also corroborated by TEM analysis. In Fig. 2 are shown TEM images of the K88 (D) and the NF (D') bacteria after the incubation with the CGMP-10/AuNP conjugate. It can be clearly observed the presence of AuNPs (small black points) attached to the K88 bacteria while by contrary, there are not nanoparticles observed in the case of the NF bacteria, evidencing the high affinity of the CGMP-10 peptide for the fimbriae. Such an interaction is probably related to the strain-depend behavior. CGMP-10 contains 3 glycosylation sites with a heterogeneous array of glycans, based on a core of Galβ1→3GalNAc (Brody, 2000; Rhoades et al., 2005). These glycans carrying terminal N-acetylneuraminic acid residues (commonly referred to as sialic acids) are known to act as receptors for several pathogens, including enterotoxigenic and enteroaggregative *E. coli* strains, allowing thus the interaction with the fimbriae *E. coli*.

4. Conclusions

A simple proof of concept electrochemical theranostic platform based on the use of gold nanoparticles with interest for the study of the effect of k-casein derived peptides as inhibitors of bacterial adhesion is developed. The peptide modified gold nanoparticles are firstly characterized by TEM, UV–vis, and Z-potential so as to ensure stable, size-homogenous and well dispersed nanoinhibitors. The prepared peptide modified nanoparticles are used for the evaluation of the interaction between the peptides and the K88 fimbriae bacteria (K88). The hydrogen evolution reaction (occurred onto screen-printed carbon electrodes) induced by gold nanoparticles used also as carriers of inhibitors is followed by a simple chronoamperometric measurement at an applied fixed potential. The efficiency of this proof of concept theranostic system is also evaluated using another class of bacteria (NF) that does not present fimbriae onto its surface. The obtained results show that gold nanoparticles can be easily loaded with k-casein derived, driven toward fimbria bacteria and electrochemically detected distinguishing the fimbriae (K88) from non-fimbriae (NF) bacteria.

The developed proof of concept system, given its simplicity and fast development possibility, could be with interest for several other biotechnological applications including food, health and pharmaceutical fields.

Acknowledgments

We acknowledge MEC (Madrid) for the projects AGL2009-07328 and MAT2011-25870 and the NATO Science for Peace and Security Programme's support under the project SfP 983807.

Appendix A. Supporting information

Supplementary data associated with this article can be found in the online version at http://dx.doi.org/10.1016/j.bios.2012.07.042.

References

Aimutis, W.R., 2004. Journal of Nutrition 134, 989S–995S.
Aragay, G., Pons, J., Merkoçi, A., 2011. Journal of Materials Chemistry 21, 4326.
Barreto, J.A., O'Malley, W., Kubeil, M., Graham, B., Stephan, H., Spiccia, L., 2011. Advanced Materials 23, H18–H40.
Blecher, K., Nasir, A., Friedman, A., et al., 2011. Virulence 2, 395.
Brody, E.P., 2000. British Journal of Nutrition 84, S39–S46.
Chauhan, V.P., Stylianopoulos, T., Martin, J.D., Popović, Z., Chen, O., Kamoun, W.S., Bawendi, M.G., Fukumura, D., Jain, R.K., 2012. Nature Nanotechnology 7, 383–388.
Dreaden, E.C., Alkilany, A.M., Huang, X., Murphy, C.J., El-Sayed, M.A., 2012. Chemical Society Reviews 41, 2740–2779.
Dykman, L., Khlebtsov, N., 2012. Chemical Society Reviews 41, 2256–2282.
De la Escosura-Muñiz, A., Ambrosi, A., Merkoçi, A., 2008. TrAC, Trends in Analytical Chemistry 27, 568–584.
De la Escosura-Muñiz, A., Parolo, C., Merkoçi, A., 2010a. Materials Today 13, 24–34.
De la Escosura-Muñiz, A., Maltez-da Costa, M., Sánchez-Espinel, C., Díaz-Freitas, B., Fernández-Suarez, J., González-Fernández, Á., Merkoçi, A., 2010b. Biosensors and Bioelectronics 26, 1710–1714.
De la Escosura-Muñiz, A., Sánchez-Espinel, C., Díaz-Freitas, B., González-Fernández, A., Maltez-da Costa, M., Merkoçi, A., 2009. Analytical Chemistry 81, 10268–10274.
De Medina, F.S., Daddaoua, A., Requena, P., Capitán-Cañadas, F., Zarzuelo, A., Dolores Suárez, M., Martínez-Augustin, O., 2010. Proceedings of the Nutrition Society 69, 454–462.
Giljohann, D.A., Seferos, D.S., Daniel, W.L., Massich, M.D., Patel, P.C., Mirkin, C.A., 2010. Angewandte Chemie International Edition 49, 3280–3294.
Huang, L., Guo, Y., Peng, Z., Porter, A.L., 2011. Technology Analysis and Strategic Management 23, 527–544.
Jans, H., Huo, Q., 2012. Chemical Society Reviews 41, 2849–2866.
Jiang, X., Jiang, J., Jin, Y., Wang, E., Dong, S., 2005. Biomacromolecules 6, 46–53.
Kawasaki, Y., Isoda, H., Tanimoto, M., Dosako, S., Idota, T., Ahiko, K., 1992. Bioscience Biotechnology and Biochemistry 56, 195–198.
Lane, J.A., Mehra, R.K., Carrington, S.D., Hickey, R.M., 2010. International Journal of Food Microbiology 142, 1–13.
Liu, Y., Guo, R., 2009. Journal of Colloid and Interface Science 332, 265–269.
Madec, F., Bridoux, N., Bounaix, S., Cariolet, R., Duval-Iflah, Y., Hampson, D.J., Jestin, A., 2000. Veterinary Microbiology 72, 295–310.
Malkoski, M., Dashper, S.G., O'Brien-Simpson, N., Talbo, G.H., Macris, M., Cross, K.J., Reynolds, E.C., 2001. Antimicrobial Agents and Chemotherapy 45, 2309–2315.
Merkoçi, A., 2010. Biosensors and Bioelectronics 26, 1164–1177.
Mohanraj, V.J., Chen, Y., 2006. Tropical Journal of Pharmceutical Research 5, 561–573.
Nakano, T., Inoue, I., Koyama, I., Kanazawa, K., Nakamura, K.-I., Narisawa, S., Tanaka, K., Akita, M., Masuyama, T., Seo, M., Hokari, S., Katayama, S., Alpers, D.H., Millán, J.L., Komoda, T., 2007. American Journal of Physiology Gastrointestinal and Liver Physiology 292, G1439–G1449.
Peer, D., Karp, J.M., Hong, S., Farokhzad, O.C., Margalit, R., Langer, R., 2007. Nature Nanotechnology 2, 751–760.
Perfézou, M., Turner, A., Merkoçi, A., 2011. Chemical Society Reviews 41, 2606–2622.
Pérez-López, B., Merkoçi, A., 2011. Analytical and Bioanalytical Chemistry 399, 1577–1590.
Reis, S., Moutinho, C.G., Matos, C., de Castro, B., Gameiro, P., Lima, J.L.F.C., 2004. Analytical Biochemistry 334, 117–126.
Rhoades, J.R., Gibson, G.R., Formentin, K., Beer, M., Greenberg, N., Rastall, R.A., 2005. Journal of Dairy Science 88, 3455–3459.
Sharon, N., Gallagher, J., 2009. Current Opinion in Structural Biology 19, 495–497.
Shoaf-Sweeney, K.D., Hutkins, R.W., 2009. Advances in Food and Nutrition Research 55, 101–161.

Sun, R., Anderson, T.J., Erickson, A.K., Nelson, E.A., Francis, D.H., 2000. Infection and Immunity 68, 3509–3515.
Thielbeer, F., Donaldson, K., Bradley, M., 2011. Bioconjugate Chemistry 22, 144–150.
Turkevich, J., Cooper Stevenson, P., Hillier, J., 1951. Discussions of the Faraday Society 11, 55–75.
Walstra, P., 1999. International Dairy Journal 9, 189–192.
Xu, Z.P., Zeng, Q.H., Lu, G.Q., Yu, A.B., 2006. Chemical Engineering Science 61, 1027–1040.
Xue, X., Wang, F., Liu, X., 2011. Journal of Materials Chemistry 21, 13107–13127.
Yang, F., Jin, C., Subedi, S., Lee, C.L., Wang, Q., Jiang, Y., Li, J., Di, Y., Fu, D., 2012. Cancer Treatment Reviews 38, 566–579.